# How are the Lower Lying Atoms Imaged Brighter than the Higher Lying Ones in the STM Experiments?

**Dongwoon Jung**

*Department of Chemistry, Wonkwang University, Iksan, Jeonbuk 570-749, Korea*
*Received January 2, 2001*

Unexpectedly, the brightest row was known to represents the lowest lying Te atoms in the STM image of NbTe2. Projected density of states and crystal orbital overlap population show that the $5p_z$ orbital of the lowest lying Te(2) atom does not interact with the 4d orbital of Nb strongly so that the $5p_z$ band remains in the vicinity of the Fermi energy. Consequently the lowest lying Te(2) atoms contribute higher electron density near the Fermi energy which in turn exhibits brightest image in the STM experiments.

**Keywords :** Transition metal dichalcogenides, STM, AFM, Electron density, Fermi energy.

## Introduction

Since its advent in 1982, scanning tunneling microscopy (STM)[1] has become one of the powerful tool for surface analysis. It probes a tunneling current between a sharp metallic tip and a conducting surface. The current changes in the constant height mode or the height changes in the constant current mode detected while scanning over a surface are converted into an bright and dark images. Provided that the tip-surface interaction is negligible, an STM image of the surface is determined by the partial density plot of the surface, $\rho(r_o, e_F)$.[2] The local density of states (LDOS) of the surface atoms at the Fermi level, $\rho(e_F)$, is related to $\rho(r_o, e_F)$ as follows:

$$\rho(e_F) = \int_{-\infty}^{\infty} \rho(r_o, e_F)\, dr_o^3$$

This implies that the brightness of an STM image depends on two factors; the electronic factor which means that the surface electron density associated with the energy levels in the vicinity of the Fermi energy, $e_F$ of the material, and the geometric factor that represents the distance between the tip and surface, $r_o$. Generally, the geometric factor dominates in determining the brightness of STM images since the number of tunneling electrons decreases exponentially as the tip-to-surface distance increases. It is expected therefore that the protruded atoms on the surface are expressed brighter in STM images. However, the electronic factor can govern the brightness of the STM image when the height difference of the atoms on surface is not so big.

Transition metal dichalcogenides $MX_2$ (M = transition metal, X = chalcogen) are layered compounds in which each layer is weakly bound by van der Waals force. Each layer is, therefore, easily cleaved and the structure of the surface after the cleavage is not changed compared with that of the bulk. This is the reason why the surfaces of transition metal dichalcogenides are widely used for scanning tunneling microscopy and atomic force microscopy (AFM) experiments. A layer in $MX_2$ is composed of three sheets, in which a metal one is sandwiched by two chalcogen ones. Under the given structure, therefore, the tip faces a chalcogen sheet first when it scans the cleaved surface of $MX_2$. Although the lobe of a metal d-orbital points to the direction perpendicular to the basal plane (*i.e.*, the plane of the cleaved layer), the tip feels the orbitals of chalcogens more strongly since the height difference between the chalcogen sheet and the metal one is quite large. Bright rows in the STM images of $MX_2$, therefore, are expected to be associated with the chalcogen atoms. This is true for many $MX_2$ compounds including $NbTe_2$,[3] $WTe_2$,[3] $ReS_2$,[4] and $ReSe_2$,[5] etc. Between the chalcogen atoms in the same sheet, however, the height difference between chalcogen atoms are rather small compared with that between the chalcogens and metal atoms. Consequently the brightness of the STM image of different chalcogen atoms is not always proportional to the extent of the protrusion. In other words the brightness of the STM image of a $MX_2$ compound is related to the electron density in the vicinity of the Fermi energy of the material. This phenomenon has been found in many transition metal dichalcogenides, but the reason why the phenomenon arises has not been systematically investigated yet. We consider $NbTe_2$ as an example to examine the reason. In $NbTe_2$ the STM images of the lowest lying Te atoms are brighter than those of protruded Te atoms. This tells us that the higher electron density of the lowest lying Te atoms in the vicinity of the Fermi energy overcomes the geometric disadvantages. In this paper the reason how the electron density in the vicinity of the Fermi energy for the lowest lying atom can be higher than that for the protruded atom is investigated by examining the crystal and electronic structures of $NbTe_2$ using tight-binding band calculations based on the extended Huckel method.[6]

## Structure of $NbTe_2$

The d-electron count of Nb in 1T-$NbTe_2$ is not $d^1$ but is close to $d^{4/3}$ because of a partial Te-to-Nb electron transfer.[7] As a consequence of increasing the number of electrons the structure of the compound with the electron count of $d^{4/3}$ is known to exhibit a ribbon-chain pattern in the metal sheet.[8]

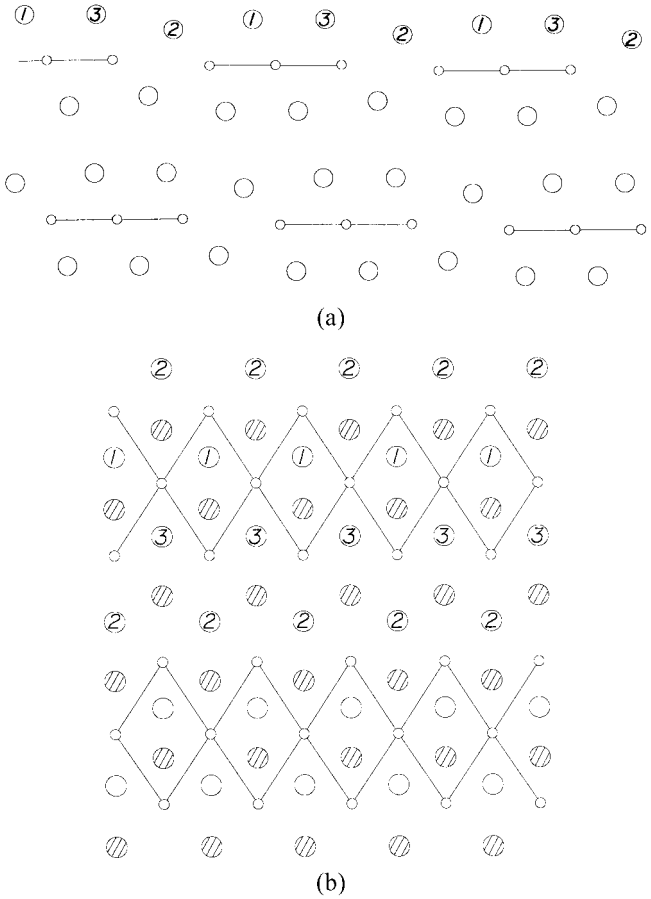


**Figure 1**. (a) Side projection view of two adjacent $NbTe_2$ layer along the y-direction. The numbers 1, 2, and 3 represent the Te(1), Te(2), and Te(3) atoms, respectively. (b) Top projection view of a single $NbTe_2$ layer along the z-direction.

$NbTe_2$ possesses exactly the expected structure in which two non-equivalent Nb atoms and three non-equivalent Te atoms exist. The side projection view along the y-direction clearly shows that there are height difference between two non-equivalent Nb atoms and between three non-equivalent Te atoms (see Figure 1a). Each ribbon chain is not completely flat but is slightly canted from the basal plane (*i.e.*, xy-plane) so that two different Nb atoms exist with the height difference of . Likewise three distinguished Te atoms arise according to the distortion of metal sheets with the height difference from the basal plane. Hereafter we denote the most protruded Te atom as Te(3), the lowest lying Te atom as Te(2), and the middle positioned Te atom as Te(1) for convenience. The most protruded Te(3) atom lies higher than the Te(1) and Te(2) by 0.082 and 0.585 Å, respectively. According to the structural results, one can expect that Te(3) atoms will be brightest in the STM experiments. The top projection view (*i.e.*, along the z-direction) of a single $NbTe_2$ layer is shown in Figure 1b where the small and large circles represent Nb and Te atoms, respectively. The Te atoms lying beneath the metal sheet are indicated by shading, and the metal-metal bonds are connected by solid lines. Note that Te(1), Te(2) and Te(3) atoms are surrounded by three Nb atoms to make short Nb-Te(1), Nb-Te(2) and Nb-Te(3) bonds. Similarly, Each Nb atom is surrounded by six Te atoms to form $NbTe_6$ octahedra which are edge-shared.

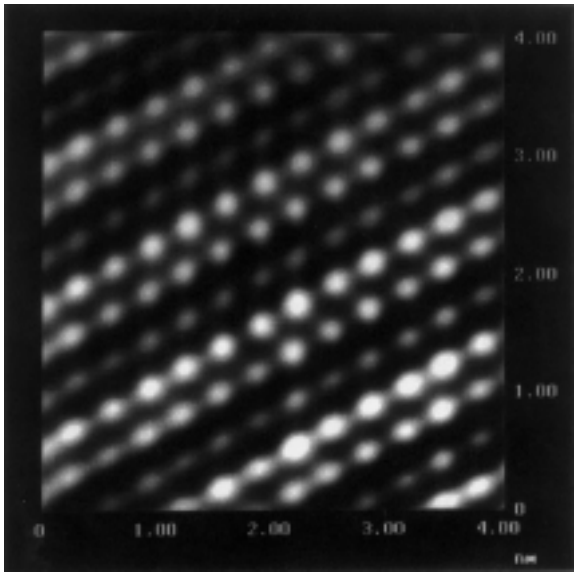


**Figure 2**. Atomic scale Fourier transformed STM image of $NbTe_2$.

## LDOS and COOP Calculations

Figure 2 shows the Fourier transformed STM image for the cleaved surface of $NbTe_2$.[3] It is clear from the image that there are three rows (*i.e.*, dim, brighter, and brightest rows) which are continuously repeating. As mentioned earlier the brightest row in the STM image of $NbTe_2$ is expected to represent Te(1) atoms since they are most protruded. However, the local electron density calculation showed that the dim, brighter, and brightest rows represent Te(1), Te(3), and Te(2) rows, respectively. Now the reason why the lowest lying Te(2) atoms are imaged brightest in the STM experiments is the interesting phenomenon to be investigated. As shown in Figure 1b, Te(2)···Nb bond distances are slightly longer than Te(1)···Nb and Te(3)···Nb bond distances (*i.e.*, 2.841 Å and 2.897 Å for Te(2)···Nb, 2.695 Å and 2.846 Å for Te(3)···Nb and 2.763 Å and 2.885 Å for Te(1)···Nb, respectively). The difference in bond distances may cause the difference in the amount of the orbital interactions between Nb 4d and Te 5p and finally the electron density in the vicinity of the Fermi energy. Figure 3a illustrates the projected density of states (PDOS) curve for the $5p_x$ and $5p_y$ orbitals of Te atoms in the vicinity of the Fermi energy calculated for a single $NbTe_2$ layer. Essentially the electron density contributions from three different Te atoms around the Fermi energy are similar. Also shown in Figure 3a is that the positions of the $5p_x$ and $5p_y$ block bands of Te(1), Te(3), and Te(2) arises at the same energy regions which means that the orbital interactions in the vicinity of the Fermi energy between Te 5p and Nb 4d along the x and y directions is almost same for Te(1), Te(2), and Te(3) atoms. However, the $5p_z$ block band of Te(2) atom is shifted to the higher energy region than those of Te(1) and

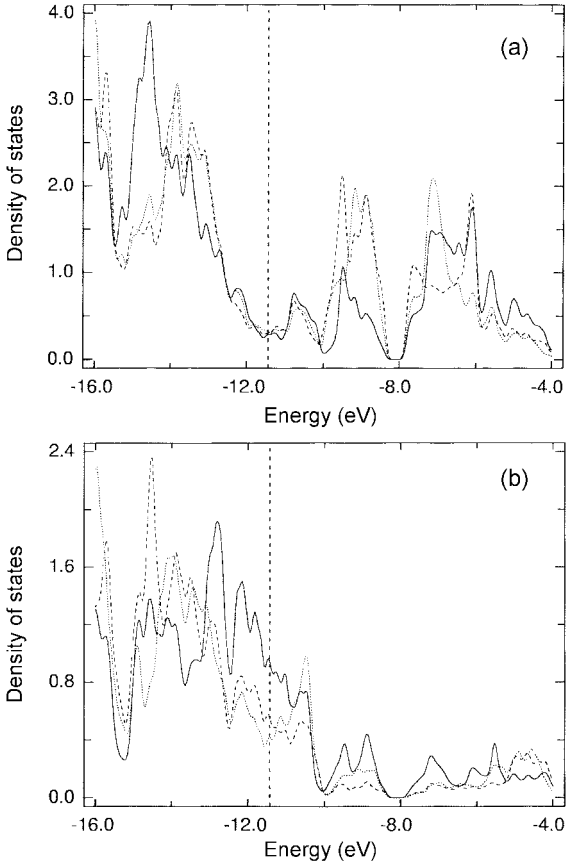


**Figure 3**. (a) Projected density of states plot for the $5p_x$ and $5p_y$ of Te(1) (dashed line), Te(2) (solid line), and Te(3) (dotted line). (b) Projected density of states plot for the $5p_z$ of Te(1) (dashed line), Te(2) (solid line), and Te(3) (dotted line). The vertical line represents the Fermi energy.

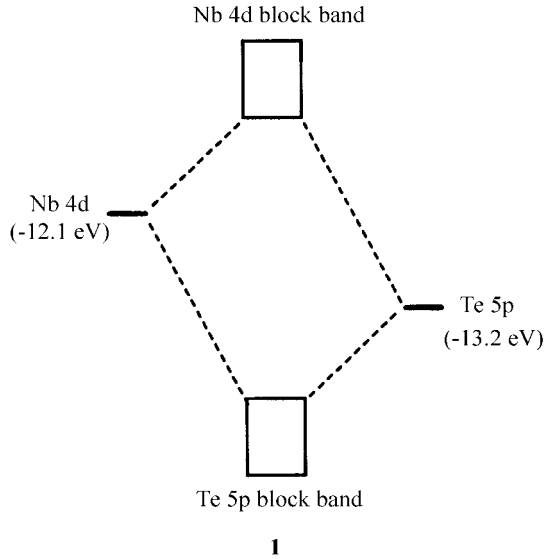


**1**

Te(3) atoms. As a consequence the contribution from the $5p_z$ orbitals of the lowest lying Te(2) atoms is unexpectedly much stronger than those from the higher lying Te(1) and Te(3) atoms near the Fermi energy, as shown in Figure 3b. What does make the difference in energy region associated with $5p_z$ bands of Te(1), Te(2), and Te(3)? When two orbitals $\Phi_1$ and $\Phi_2$ interact, two new crystal orbitals $\Psi_a$ and $\Psi_b$ are formed as briefly illustrated in **1**.

The stronger the $\Phi_1$ and $\Phi_2$ interact, the larger the $\Psi_a$ and $\Psi_b$ split. Of course, the characters of new $\Psi_a$ and $\Psi_b$ are closer to $\Phi_1$ and $\Phi_2$, respectively. In $NbTe_2$ $\Phi_1$ and $\Phi_2$ represent Nb 4d (-12.1 eV) and Te 5p (-13.2 eV) orbitals, respectively. PDOS results show that $5p_x$ and $5p_y$ of Te(1), Te(2), and Te(3) interact with Nb 4d with similar strength. But $5p_z$ of Te(1) and Te(3) interact with Nb 4d rather strongly compared with the interaction between $5p_z$ of Te(2) and Nb 4d. Therefore, the energy region for $\Psi_b$ bands (*i.e.*, $5p_z$ bands) of Te(1) and Te(3) go down further while that of Te(2) remains around the original energy region of Te 5p. The PDOS curve (see Figure 3b) clearly show that the energy region of the $5p_z$ block bands of Te(3), Te(2), and Te(1) after the interaction with Nb 4d are -14.0~-13.0 eV, -13.0~-10.2 eV, and -14.7~-12.5 eV, respectively.

The crystal orbital overlap population (COOP) curve calculated for the Te(1)⋯Nb, Te(2)⋯Nb, and Te(3)⋯Nb bonds support the very weak interaction of Te(2) atoms with Nb, as shown in Figure 4. Near the Fermi energy the COOP of Te(2)⋯Nb bonds are weak compared with those of higher lying Te(1) and Te(3) atoms. The non-bonding character in Te(2) $5p_z$ is explained in terms of bond distances and symmetry. As depicted earlier, Te(2)⋯Nb distances are slightly longer than those of Te(1)⋯Nb and Te(3)⋯Nb. The longer bonds in Te(2)⋯Nb first cause the weak interaction between the $5p_z$ of Te(2) and 4d of Nb and second destroy the symmetry along the z-direction which in turn, cause the decrease of interaction between the $5p_z$ of Te(2) and 4d of Nb. In the long run the 5p of the lowest lying Te(2) atom does not interact with the 4d of Nb strongly in the vicinity of the Fermi energy so that the band remains near the Fermi energy and finally results in the higher electron density. Therefore, the electron density contribution from total 5p is stronger for Te(2) than the other two Te atoms, and the STM image is brighter for Te(2) atom. As a result, it is clear that the lower lying atoms can be imaged brighter than the higher lying

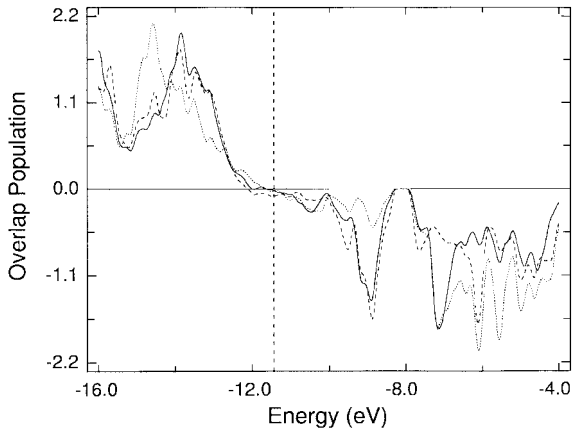


**Figure 4**. Crystal orbital overlap population plot for the Te(1)⋯Nb (dashed line), Te(2)⋯Nb (solid line), and Te(3)⋯Nb (dotted line). The vertical line represents the Fermi energy.

ones when the electron density in the vicinity of the Fermi energy is higher, and the height difference is not large. Although the reason for the unexpected result in the STM image of $NbTe_2$ is examined in this study, the results can be applied to many $MX_2$ compounds to be imaged by the STM experiments.

## Conclusions

In $NbTe_2$ the STM images of the lowest lying Te atoms are brighter than those of more protruded Te atoms. The PDOS curve for the $5p_x$ and $5p_y$ orbitals of Te atoms in the vicinity of the Fermi energy calculated for a single $NbTe_2$ layer is essentially similar despite of the height differences in three Te atoms. However, the electron density contribution from the $5p_z$ orbitals of the lowest lying Te(2) atoms is unexpectedly much stronger than those from the higher lying Te(1) and Te(3) atoms near the Fermi energy. The reason for the unexpected results is that the 5p of the lowest lying Te(2) atom does not interact with the 4d of Nb strongly in the vicinity of the Fermi energy so that the band remains near the Fermi energy and finally results in the higher electron density. This result can be applied to many $MX_2$ compounds to be imaged by the STM experiments.

**Acknowledgment**. This work was supported by grant 2000-1-12200-003-2 from the Basic Research Program of the KOSEF and partly by wonkwang university research fund made in 1999.

## References

1. Binnig, G.; Rohrer, H.; Gerber, Ch.; Weibel, E. *Phys. Rev. Lett.* **1982**, *49*, 57.
2. (a) Tersoff, J.; Hamann, D. R. *Phys. Rev. B* **1985**, *31*, 805. (b) Tersoff, J. *Phys. Rev. Lett*. **1986**, *57*, 440.
3. Bengel, H.; Cantow, H.-J.; Magonov, S. N.; Jung, D.; Ren, J.; Whangbo, M.-H. *New J. Chem*. **1996**, *20*, 287
4. Kelty, S. P.; Ruppert, A. F.; Chianelli, R. R.; Ren, J.; Whangbo, M.-H. *J. Am. Chem. Soc*. **1994**, *116*, 7857.
5. Parkinson, B. A.; Ren, J.; Whangbo, M.-H. *J. Am. Chem. Soc*. **1991**, *113*, 7833.
6. (a) Whangbo, M.-H.; Hoffmann, R. *J. Am. Chem. Soc*. **1978**, *100*, 6093. (b) Ammeter, J. H.; Thibeault, J. C.; Hoffmann, R. *J. Am. Chem. Soc*. **1978**, *100*, 3686.
7. Canadell, E.; Jobic, S.; Brec, R.; Rouxel, J.; Whangbo, M.-H. *J. Solid State Chem*. **1992**, *99*, 189.
8. (a) Brown, B. E. *Acta Cryst.* **1966**, *20*, 264. (b) Magonov, S. N.; Whangbo, M.-H. *Adv. Mater.* **1994**, *6*, 355.